Citation: Molecular Therapy—Nucleic Acids (2016) 5, e390; doi:10.1038/mtna.2016.93
Official journal of the American Society of Gene & Cell Therapy
www.nature.com/mtna

Antisense Oligonucleotide Mediated Splice Correction of a Deep Intronic Mutation in *OPA1*

Tobias Bonifert[1,2], Irene Gonzalez Menendez[1], Florian Battke[3], Yvonne Theurer[4,5], Matthis Synofzik[4,5], Ludger Schöls[4,5] and Bernd Wissinger[1]

Inherited optic neuropathies (ION) present an important cause of blindness in the European working-age population. Recently we reported the discovery of four independent families with deep intronic mutations in the main inherited optic neuropathies gene *OPA1.* These deep intronic mutations cause mis-splicing of the *OPA1* pre-messenger-RNA transcripts by creating cryptic acceptor splice sites. As a rescue strategy we sought to prevent mis-splicing of the mutant pre-messenger-RNA by applying 2′O-methyl-antisense oligonucleotides (AONs) with a full-length phosphorothioate backbone that target the cryptic acceptor splice sites and the predicted novel branch point created by the deep intronic mutations, respectively. Transfection of patient-derived primary fibroblasts with these AONs induced correct splicing of the mutant pre-messenger-RNA in a time and concentration dependent mode of action, as detected by pyrosequencing of informative heterozygous variants. The treatment showed strong rescue effects (~55%) using the cryptic acceptor splice sites targeting AON and moderate rescue (~16%) using the branch point targeting AON. The highest efficacy of Splice correction could be observed 4 days after treatment however, significant effects were still seen 14 days post-transfection. Western blot analysis revealed increased amounts of OPA1 protein with maximum amounts at ~3 days post-treatment. In summary, we provide the first mutation-specific *in vitro* rescue strategy for OPA1 deficiency using synthetic AONs.

Molecular Therapy—Nucleic Acids (2016) **5**, e390; doi:10.1038/mtna.2016.93; published online 22 November 2016
Subject Category: Antisense oligonucleotides and Therapeutic proof-of-concept

Introduction

Inherited optic neuropathies (ION) are a major cause of hereditary blindness in infants of Western populations with currently no causative treatment available. Apart from mutations in the mitochondrial genome causing Leber's hereditary optic neuropathy, in total six nuclear genes have been identified to cause nonsyndromic optic neuropathies: *OPA1* (refs. 1,2), *OPA3*(ref. 3), *OPA7* (*TMEM126*),[4] *ACO2*(ref. 5), *WFS1*(refs. 6,7), and *RTN4IP1*(ref. 8). The large GTPase OPA1 is anchored to the inner mitochondrial membrane and has been ascribed to participate in various functions, including mitochondrial DNA maintenance,[9] tethering of the cristae junctions[10] and most importantly: fusion of the inner mitochondrial membrane.[11] Molecular analyses of patients with heterozygous *OPA1* mutations suggest haploinsufficiency as the most predominant pathomechanism underlying *OPA1* associated retinal ganglion cell loss in affected subjects.[12] Although *OPA1* accounts for more than 60% of all cases in dominant optic atrophies,[13] the remaining share of cases is not necessarily explained by mutations in novel genes. We could recently show that some of these unresolved IONs result from deep intronic point mutations (DIMs) in *OPA1* (ref. 14). The mutations c.610+360G>A and c.610+364G>A (nucleotide positions referring to transcript NM_130837.1) found in four independent families are located within intron 4b of *OPA1* and each activate a cryptic splice acceptor site and one of two pre-existing splice donor sites (**Figure 1**) causing the inclusion of intronic sequences between exons 4b and 5 of the mutant mRNA. By allelic discrimination on the transcript level we could demonstrate that mis-splicing is constitutive for the mutant alleles while correctly spliced *OPA1* transcripts exclusively derive from the alternate alleles. Both DIMs induce premature termination codons (see **Supplementary Figure S1**) and we have demonstrated by puromycin treatment of patient-derived fibroblasts that these stop codons induce nonsense-mediated mRNA decay. Furthermore, we could show reduced steady-state levels of the mutant transcript in fibroblasts of patients with the c.610+364G>A along with a marked reduction of OPA1 protein levels compared with controls (In the following we refer to c.610+364G>A as: DIM 364).

Antisense oligonucleotides (AON) are single stranded 8-50mer DNA or RNA molecules that engage in Watson-Crick basepairing with (pre-)mRNA or DNA and have attracted attention as target-specific drugs. Depending on target site and backbone chemistry, these AONs either induce RNAseH dependent degradation of the bound transcript or prevent ribosomal/spliceosomal recognition of the binding site, causing translational block and exon skipping, respectively. For a comprehensive review on AON chemistry, mechanisms and medical relevance see Sharma and Watts (2015) (ref. 15).

[1]Molecular Genetics Laboratory, Institute for Ophthalmic Research, Center for Ophthalmology, University of Tübingen, Tübingen, Germany; [2]Graduate School of Cellular and Molecular Neuroscience, University of Tübingen, Tübingen, Germany; [3]CeGaT GmbH, Tübingen, Germany; [4]Department of Neurodegenerative Diseases and Hertie-Institute for Clinical Brain Research, University of Tübingen, Tübingen, Germany; [5]German Center for Neurodegenerative Diseases (DZNE), Tübingen, Germany. Correspondence: Bernd Wissinger, Molecular Genetics Laboratory, Institute for Ophthalmic Research, Center for Ophthalmology, University of Tübingen, Röntgenweg 11, 72076 Tübingen, Germany. E-mail: wissinger@uni-tuebingen.de
Keywords: antisense oligonucleotides; deep intronic mutation; OPA1; optic neuropathies; splice correction
Received 13 June 2016; accepted 13 September 2016; published online 22 November 2016. doi:10.1038/mtna.2016.93

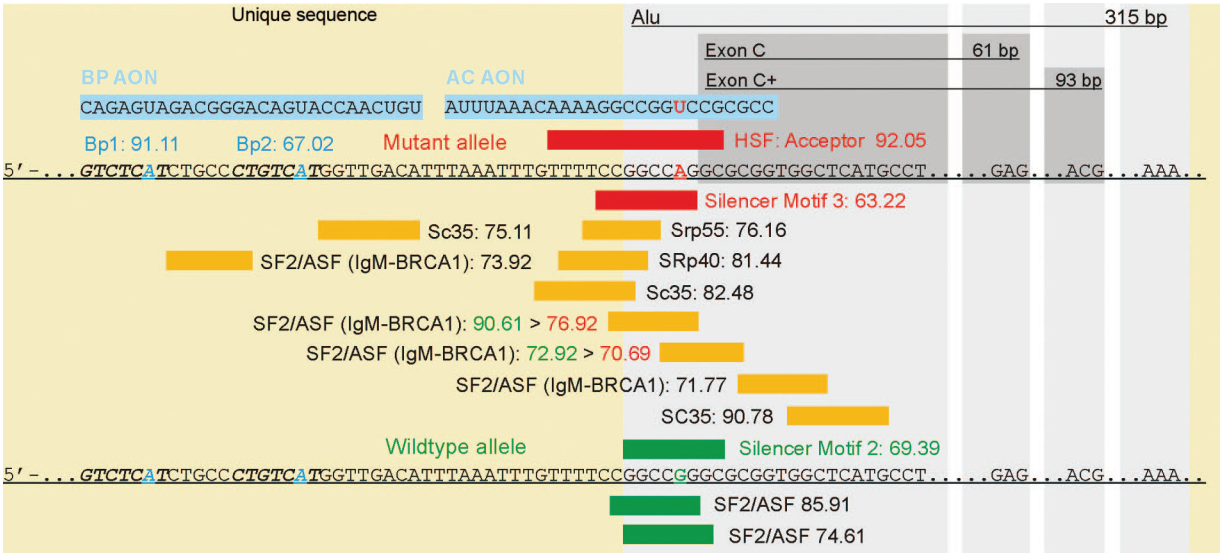

Figure 1 Binding sites for AONs and predicted SF binding sites on the c.610+364G>A mutant allele and the corresponding wildtype allele. The sequence of the c.610+364G>A mutant allele is shown on top in comparison with the corresponding wildtype allele (bottom) as present in the patient fibroblasts. The mutation (red A) is located 5 bp downstream of the 5′ terminus of an Alu element (315 bp, highlighted in light gray) and two nucleotides upstream of exon c (61/93 bp, dark gray box). HSF predicted two branch points (blue adenosines) and 13 Exon Splice Enhancer motives (yellow boxes), two of them with higher affinity to the wildtype allele and two SF2/ASF motives that are specific for the WT allele (green boxes). One silencer motif was slightly weakened by the DIM. Indicated numbers represent HSF predicted scores for SF affinity at the respective binding sites. AC AON and BP AON are highlighted in blue. AON, antisense oligonucleotides; BP, branch point; DIM, deep intronic mutation; HSF, human splicing finder; SF, splice factor; WT, wild type.

Currently, only two antisense-based therapeutics have been approved by the FDA, both of which function via an RNAseH mediated mechanism.[16,17] Concerning splice-switching AONs, Drisapersen and Eteplirsen, chemically modified AONs that induce skipping of mutant exon 51 in the Duchenne Muscular Dystrophy (*DMD*) gene have reached clinical trials for the treatment of DMD.[18,19] Furthermore, splice-switching AONs may be used to suppress inclusion of cryptic exons activated by DIMs. This approach has been proven efficient in earlier *in vitro* studies targeting retinal disease mutations *e.g.*, the DIM c.2991+1655A>G in *CEP290*, a common mutation associated with Leber congenital amaurosis.[20,21]

In this study, we designed and evaluated two AONs that efficiently prevent mis-splicing of *OPA1* DIM-transcripts in patient-derived primary fibroblasts, resulting in increased levels of correctly spliced transcripts and an elevated amount of OPA1 protein. In the context of haploinsufficiency being the most common pathomechanism in *OPA1*-associated optic atrophy, our study provides proof of concept for AON technology to facilitate increasing OPA1 protein levels in DIM carriers, which is expected to have therapeutic effects.

Results

Design of antisense oligonucleotides

In order to overcome mis-splicing induced by DIM 364, we designed two different AONs: The AC AON (5′-CCGCGCC UGGCCGGAAAACAAAUUUA-3′) targets the cryptic acceptor site in the vicinity of DIM 364, whereas the BP AON (5′-UGUC AACCAUGACAGGGCAGAUGAGAC-3′) was meant to cover two putative branch point adenosines located 30 base pairs (bp) and 42 bp upstream of DIM 364 (**Figure 1**). As the mutation is located 5 bp downstream of the 5′end of a highly abundant Alu element, we refrained from targeting pseudoexon-internal sequences or the two alternative cryptic donor sites, both of which are located deeply within this Alu element. The off-target search listed the following features: binding of +strand or –strand, name of involved gene, position of binding site relative to gene (intergenic, intronic, and exonic), distance to nearest exon, number of mismatches and genomic position. Apart from the unmutated compound allele of *OPA1* (1 mismatch (MM) for AC AON, no MM for BP AON) the search did not uncover any off-targets for BP AON, however, it listed 11 further off-target binding sites for AC AON (see **Supplementary Table S1**). Six off-targets are on the antisense strand (with respect to the gene locus), the remaining six off-targets were: *OPA1* (intronic, 1 MM), *CEP128*, *RNU6-42P* (both intronic, 3 MM), *SCGB1D1*, *FAM21FP* and *SNORA51* (all three intergenic, 3 MM). All sense-strand binding sites are located far from adjacent exons (*CEP128*: 33172 bp, *RNU6-42P*: 4667 bp, *SCGB1D1*: 5696 bp, *FAM21FP*: 1122 bp, *SNORA51*: 7546 bp) but overlap with the 5′ends of Alu elements. To discriminate between specific and unspecific effects of the AON transfection we performed parallel experiments with a nontarget control AON (CON AON: 5′-CCUCUUACCUCAGUUACAAUUUAU-3′). Transfection efficiencies were determined using labeled AONs and 4,6-diamidino-2-2-phenylindole (DAPI) staining. Nuclear colocalization was observed in an average of ~54% of the cells (data not shown).

AC and BP AONs restore correct splicing of mutant allele

We transfected confluent patient-derived primary dermal fibroblasts (family OAK 587, patient II:2 carrying DIM 364 in heterozygous state) using the AC AON, BP AON and CON

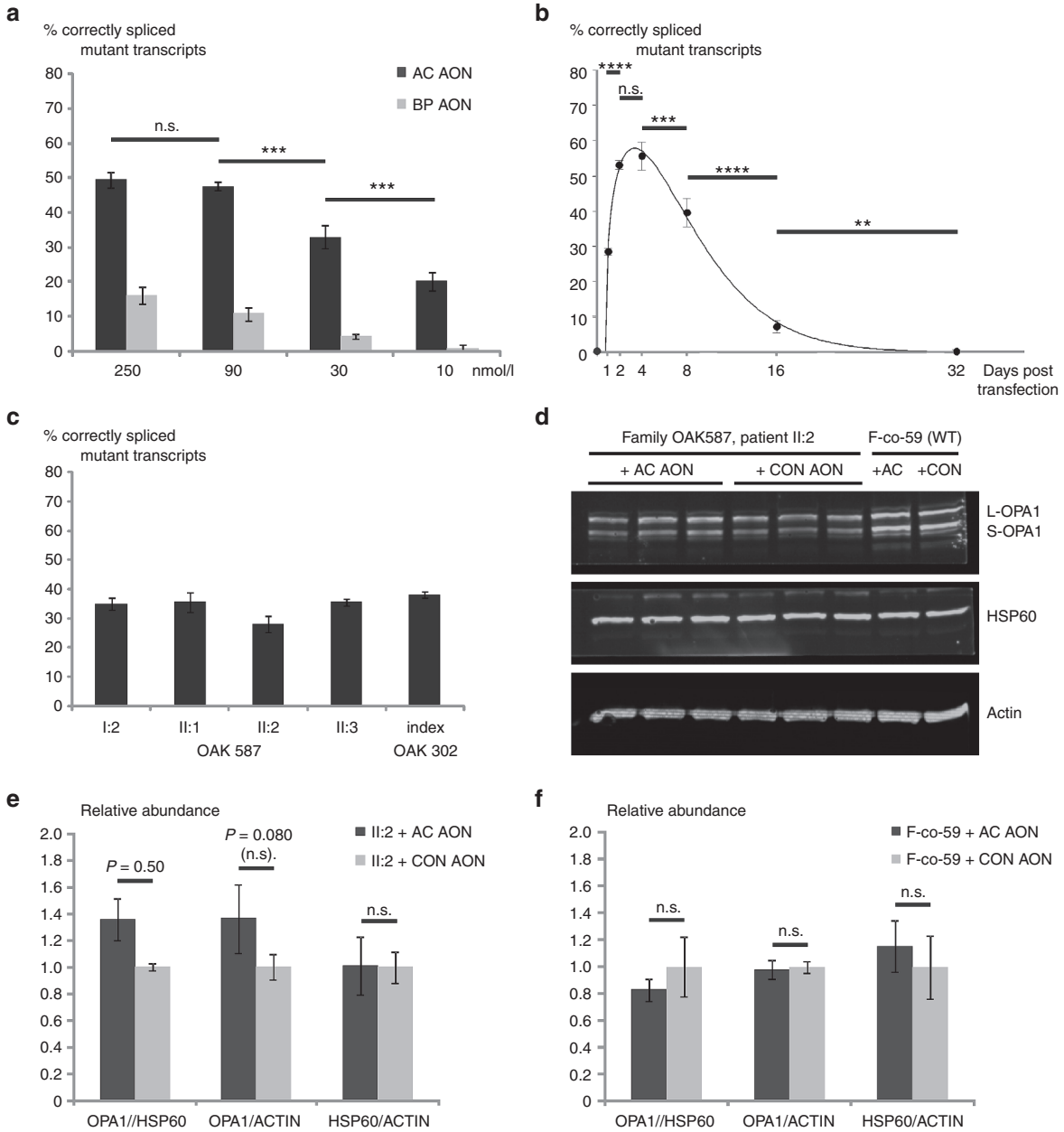

Figure 2 Efficiency of AON-mediated splice correction on RNA and protein level. (**a**) Patient fibroblasts were transfected with either AC AON, BP AON or CON AON at concentrations of 250, 90, 30, and 10 nmol/l. Cells were lysed 24 hours post-transfection. Pyrosequencing of RT products revealed rescue of the splicing defect and dose dependent splice correction in AC AON and to a lesser extent in BP AON transfected cells (Factorial ANOVA test, $P < 0.001$; AC AON ANOVA test, $P < 0.001$). No splice correction could be detected (0%) upon treatment with the CON AON. (**b**) Time course of the AON-mediated splice correction in fibroblasts treated with 20 nmol/l of AC AON at day 0. The effect peaked at day 4 and slowly decreased to ~7% at day 16 (ANOVA test $P < 0.001$; Scheffe post hoc day 0 versus day 4, $P < 0.001$; Scheffe post hoc day 4 versus day 8, $P < 0.001$; Scheffe post hoc day 8 versus day 16, $P < 0.000$). No remaining splice correction was visible at day 32 (Scheffe post hoc day 0 versus day 32, $P > 0.05$). Curve fitting by Sigma plot postulates peak efficacy of 57% at day 3.5 (four-parametric Weibull function) (**c**) Comparison of AON-mediated splice correction in fibroblasts from different mutation carriers (two independent families: OAK 587 and OAK 302). All cell cultures were transfected with 20 nmol/l of AC AON and cultured for 2 days. No correctly spliced transcripts from the mutant allele were detectable in untreated samples and splice correction was observed in all fibroblast lines. (**d**) Western blot analysis of 20 µg protein from whole cell lysates of patient and control fibroblast cultures transfected with 20 nmol/l of either AC AON or CON AON and harvested 4 days post-transfection. Immunodetection was performed with primary antibodies against OPA1 (detecting long and short OPA1 isoforms (L-OPA1 and S-OPA1), the mitochondrial marker HSP60 and the cytosolic BETA-ACTIN. OPA1 bands were stronger when treated with AC AON compared with CON AON. (**e**) Quantitative analysis of Western blots revealed significantly elevated OPA1:HSP60 ratios between patient-derived fibroblasts transfected with the AC AON and those treated with the CON AON (*U*-Mann–Whitney test, $P < 0.05$), whereas OPA1:BETA-ACTIN ratios showed a trend toward increased levels of OPA1 (student's *t*-test, $P = 0.08$). No significant change could be observed in HSP60/BETA-ACTIN ratios of the treated cells. (**f**) AON treatment of matched control fibroblasts without DIM 364 had no effect on OPA1/HSP60 or OPA1/BETA-ACTIN ratios. All error bars shown as mean+SD. ANOVA, analysis of variance; AON, antisense oligonucleotides; BP, branch point; DIM, deep intronic mutation.

AON, at different final concentrations (250, 90, 30, and 10 nmol/l). RNA extraction after 24 hours, followed by reverse transcriptase polymerase chain reaction (RT-PCR) and pyrosequencing revealed an AON-sequence, dose-dependent suppression of the mis-splicing, and rise of correctly spliced transcripts derived from the mutant allele with highest efficiencies of 49% for the AC AON ($P < 0.001$) and 16% for the BP AON, respectively (**Figure 2a**). Treatments with 250 and 90 nmol/l of AONs showed the highest efficiency with no significant difference in the two groups ($P > 0.05$), however, inducing high cell death rates with 250 nmol/l and moderate toxic effects with 90 nmol/l (data not shown). Treatment with 30 and 10 nmol/l had less pronounced effects on splice correction though cell viability in short-term culture was comparable to untreated cells. Transfection with the CON AON had no effect on *OPA1* transcript splicing. Using cocktail formulations with different absolute and relative molar quantities of BP/AC AONs in combination did not further enhance splice correction efficiencies (data not shown)

Correctly spliced mutant allele-derived transcripts can be detected for more than 14 days after AON transfection

We further refined concentration dependent toxic effects of AON treatment and accordingly transfected patient fibroblasts with AC AON at 20 nmol/l end concentration for long term investigation. Cells were transfected on day 0 and triplicate cultures were harvested at day 1, 2, 4, 8, 16, and 32 post-transfection. The splice correction over time has been extrapolated using a four-parameter Weibull function[22,23] (**Figure 2b**). The initial slope reflects the rapid AON-uptake and intracellular delivery. The strongest rescue effect was measured after 4 days with ~55% of splice-corrected transcripts ($P < 0.001$). The effect slightly declined by day 8. The half-maximum efficiency level of 27.5% is reached ~10 days post-transfection and decreases to as low as 7% after 16 days. By 1 month after treatment, at the latest, the effect of the AONs has faded, which can be considered as the combined consequences of AON degradation and cell division of transfected and nontransfected cells.

AC AON suppresses mis-splicing in different mutation carriers

To further prove the efficacy and reliability of this approach and to evaluate possible confounding effects due to differences in the genetic background, we assessed and compared splice correction in fibroblast cultures of a total of five individual subjects harboring the same DIM but of different age and gender, namely, the three affected siblings of family OAK 587 (II:1, II:2, and II:3) as well as their unaffected mother (I:2) and another male patient of the unrelated family OAK 302. All cell lines were also heterozygous for rs7624750 in *OPA1* exon 4. Upon transfection with AC AON (20 nmol/l and 48 hours culturing), all fibroblast lines responded with relatively uniform splice correction efficiencies (**Figure 2c**).

Increased OPA1 protein levels upon AC AON treatment

We wondered whether rescuing the splicing defect of mutant allele-derived transcripts likewise results in a higher OPA1 protein abundance. Indeed, semiquantitative Western blot (**Figure 2d**) revealed an increase of 35% for OPA1 protein normalized to the mitochondrial matrix protein HSP60 ($P = 0.050$) and a 36% increase normalized to cytoplasmic BETA-ACTIN ($P = 0.080$). OPA1 protein ratios showed similar increases when compared with HSP60 and BETA-ACTIN but without significance in the second comparison. This might be explained by the variability observed between the samples. Treatment was compared with cultures transfected with the nontarget CON AON (**Figure 2e**). Treatment of age, gender, and passage matched control fibroblasts showed no alteration in OPA1 levels with either AON (**Figure 2f**).

Discussion

In this study, we could demonstrate functional rescue of a deep intronic point mutation in the human *OPA1* gene by *in vitro* transfection of patient-derived fibroblasts with antisense oligonucleotides. This represents the first AON-based splice correction of a DIM in a mitochondriopathy. Two different AONs, designed to cover either the cryptic splice acceptor site or the predicted cryptic branch point, efficiently suppressed DIM 364-induced mis-splicing and restored normal splicing between exon 4b and exon 5 of *OPA1.* The relative amounts of wildtype versus mutant transcripts were measured using pyrosequencing-based allelic discrimination at a common SNP. This approach represents a novel and efficient way to precisely quantify the efficacy of AON-mediated splice correction.

The efficiency of splice correction was concentration- and time dependent and significantly higher with the AC AON compared with the BP AON. The applied concentrations perfectly fall within the range of previously reported functional AONs.[21,24,25] The highest amount of corrected mutant transcripts was at around 55% (20 nmol/l, 4 days post-transfection). Considering that a fully functional allele contributes ~50% to the gene's overall transcripts, a 55% restoration of the mutant allele corresponds to 27.5% of total transcripts, indicating a shift from 50% (only WT allele) to 77.5% (WT allele + corrected transcripts from mutant allele) of correctly spliced *OPA1* mRNAs (**Figure 3**). This amount is probably sufficient to overcome threshold levels of OPA1 that are associated with disease manifestation. A nontarget control AON had no detectable effect. AON-mediated splice correction could be proven in fibroblasts of mutation carriers of different ages and gender with similar efficiency, an important prerequisite for therapeutic strategies based on AON technologies.

Correctly spliced transcripts from the mutant allele were most abundant between days 2–4 post-transfection and decreased by a factor of ~8 until day 16. We cannot exclude that this decrease in corrected transcripts is partly caused by dilution effects due to ongoing cell division during extended culturing periods. Therefore, we reason that AON-mediated rescue might be more long-lasting in nondividing cells like retinal ganglion cells, the primary target cell population for therapy in *OPA1*-associated optic atrophy. Although patients would be required to receive therapeutic AONs repeatedly during their entire lifetime, the time intervals between repeated administrations of full-length phosphorothioate AONs might be weeks or months as indicated by experiments with exon-skipping AONs applied for *DMD*[26] and for *CEP290* (refs. 27,28).

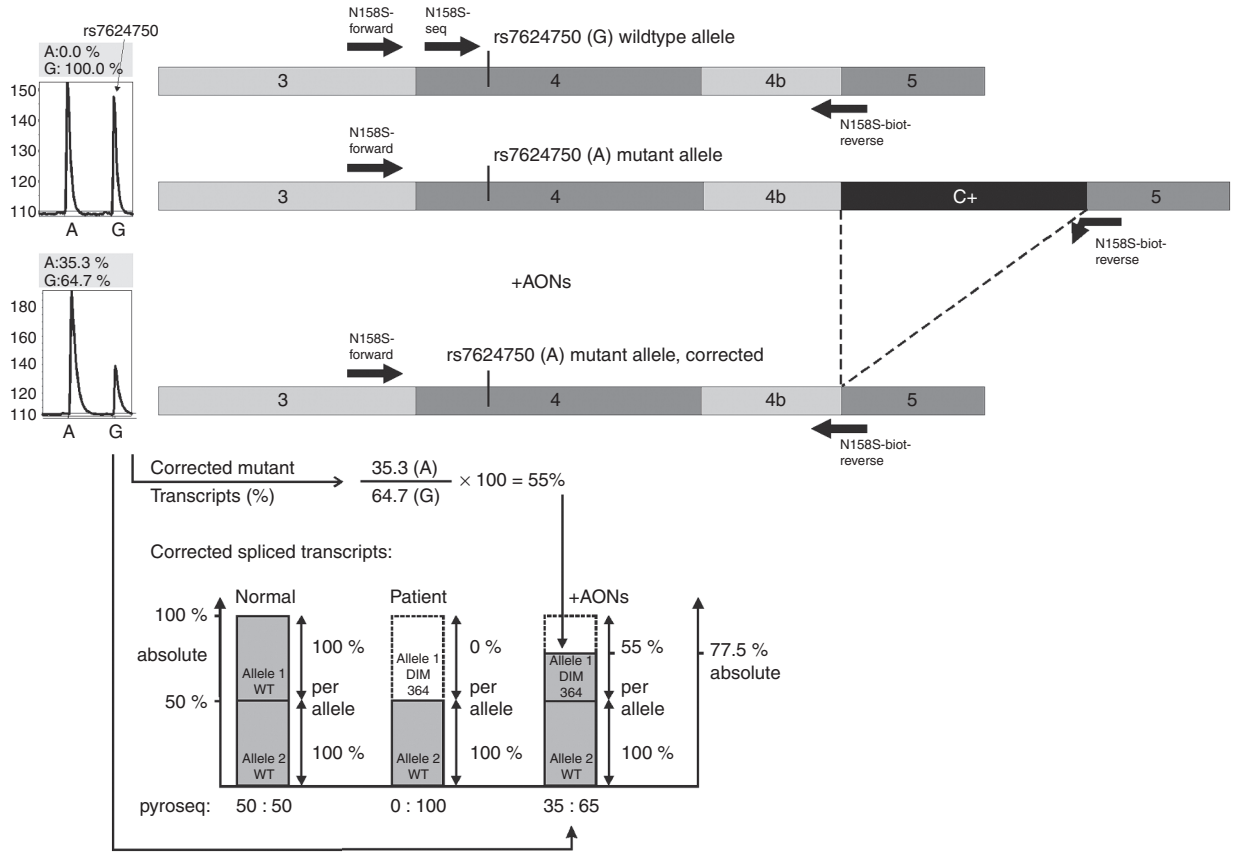

Figure 3 Pyrosequencing assay for detection of correctly spliced transcript in fibroblasts of patients with the c.610+364G>A mutation. The N158S-forward primer binds in exon 3, the N158S-biot-reverse primer at the junction of exon 4b and exon 5. This primer setting exclusively amplifies cDNA of correctly spliced *OPA1* transcripts (top bar, wildtype allele) but no transcripts with retained cryptic exon c between exons 4b/5 (middle bar, mutant allele, and upper pyrosequencing scheme). The sequencing primer (N158S-seq) binds two bases upstream of the heterozygous SNP rs7624750 in exon 4. The A allele of rs7624750 cosegregates with the mutation and cannot be detected in cDNA from mutant untreated cells using this assay. Upon AON treatment, cryptic exon c is skipped and the mutant transcript can be amplified (lower bar) and hence its allelic contribution can be measured via pyrosequencing (lower left scheme). A relative ratio of 35.3% versus 64.7% (A-allele versus G-allele) corresponds to a rescue of 55% of all mutant alleles in the cDNA of treated fibroblasts (example), which corresponds to a shift of total correctly spliced *OPA1* mRNA of 77.5% (lower graph) For further graphical illustration of the principle compare **Supplementary Figure S2**. AON, antisense oligonucleotides; cDNA, complementary DNA.

We observed strong cytotoxicity with high AON doses of 250 nmol/l and mild toxicity with 90 nmol/l. Some toxic effects at lower doses appeared only upon longer culturing periods, whereas the nontarget CON AON caused less toxicity at the same doses. Although AON-blocking of intronic long-distance interactions has been reported to interfere with canonic splicing [29], none of the predicted off-target genes was reported in context with cytotoxicity or human disease and the number of mismatches render off-target binding unlikely. The mechanism of toxicity therefore remains elusive. Partial low-affinity interactions of the AON with many independent Alu off-targets might still cause toxicity in a cumulative manner. However, in order to assess the actual biochemical cause for cytotoxicity, further investigations need to be undertaken.

The observed increase of functional *OPA1* transcripts upon AON treatment could be confirmed on the protein level using Western blotting. Relative quantification of OPA1 demonstrated an increase of OPA1 levels of around 35%.

In summary, we could show an AON-mediated rescue of a deep intronic point mutation that essentially rescues a fully penetrant splice defect and results in a prominent increase in correctly spliced *OPA1* mRNA and protein in patient-derived fibroblasts. AONs as therapeutic drugs have several clear advantages such as easy production and full chemical synthesis devoid of any sources of biological contaminations. Moreover, AONs are small molecules that easily penetrate into tissues and are taken up by neurons without complex chemical formulations or packaging vehicles.[30] For its application to treat optic atrophy and thus targeting retinal ganglion cells an administration through intravitreal injection can be envisaged. Another advantage of AON over classical gene therapy approaches is the possibility to discontinue treatment at any time, in case of side-effects which may occur. However, an indispensable prerequisite for a translation into clinical use is a further investigation of the subcellular effects of AON treatment on mitochondrial fragmentation, Cristae remodeling and susceptibility to proapoptotic stimuli, followed

by biochemical assessment of toxicity and off-target interactions. Additionally, preclinical testing in animal models with homologous mutations is needed to uncover efficacy and toxicity. Yet recent studies showed that recognition of cryptic exons is not necessarily conserved even among mammalian species.[31] A major limitation of the AON-based exon skipping technology is given through its narrow spectrum of mutations that are targeted. This specificity for a defined sequence context reduces the number of treatable patients to a few individuals, unless a certain DIM is highly prevalent in the patient population due to a founder effect, as *e.g.*, in *CEP290*-associated Leber congenital amaurosis.

This proof of concept study therefore, further highlights the importance of molecular genetic intron analyses in patient cohorts, as it provides not only the potential to uncover pathogenic mutations in unsolved ADOA families but inherently opens up possible therapeutic strategies.

Materials and methods

Antisense oligonucleotide design and composition. AONs were designed following recommendations of Aartsma-Rus and colleagues,[32] including bioinformatic tools to estimate the efficiency of potential splice-blocking AONs. We computed AON secondary structure (software: mfold[33]), free energy values of AON, target, as well as AON–AON and AON-target complexes (RNAcofold server at Vienna RNA Web Services[34]), coverage of splice factor binding sites and Branch point prediction (Human Splicing Finder[35]) and averaged single strand counts across the AON binding site (ss-count, mfold-software). In order to find and score potential off target sites of AC AON and BP AON, we used a customized script that aligned the AON sequences against the human genome (GRCh38) using Burrows-Wheeler indexing, implemented in Bowtie[36] and the standalone version of CCtop[37] without filtering for Protospacer adjacent motif (PAM) motives, conserved core sequences or sequence length restrictions. As Aartsma-Rus and colleagues have shown for AONs with 2′O-methyl-phosphorothioate backbone, three single-base mismatches prevent successful AON-target interactions.[38] Therefore we allowed three mismatches in our off-target search (Source code and instructions upon request). The AONs were synthesized by Metabion International AG (Planegg, Germany). As experimental control, we used a control oligonucleotide (CON AON) with the same chemical modifications and similar length (adapted from Gene Tools' "standard control oligo") (Gene Tools LLC, Philomath, OR). All AONs were oligoribonucleotides containing 2′O-methyl groups and a full-length phosphorothioate backbone for nuclease protection. For estimation of overall transfection efficiency, we used fluorescence-labeled versions of the CON AON with an Atto-550 dye group attached to the 5′ end during synthesis but keeping all other chemical modifications as for the nonlabeled oligonucleotides. AONs were diluted in 5 mmol/l Tris-HCl pH 7 and applied in different concentrations with polyethylenimine for transfection.

Cell culture, transfection, and RNA isolation. Primary dermal fibroblasts from patients and controls were grown in Dulbecco's modified Eagle's medium (DMEM), with 10% fetal calf serum (FCS) and 1% penicillin-streptomycin (Pen-Strep) (10,000 U/ml). The cells from patients OAK 302-index and OAK 587-I:2 were heterozygous for DIM 364, whereas the cells from patients II:1, II:2, and II:3 of the same family were compound heterozygous for DIM 364 and the variant c.1311A>G/p.I437M, NM_130837.1. One day before transfection, three confluent T175 cell culture flasks were trypsinized, the harvested cells pooled (~27 ml) and 1 ml of the cell suspension seeded in 5 ml of DMEM/FCS/Pen-Strep in T25 flasks. Bright field microscopy images were taken at 50× magnification prior to transfection and directly before lysis at three different areas of each flask, in order to verify equal cell density across and between the flasks as well as to document potential toxic effects upon AON treatment. Transfection was carried out using Polyethylenimine (PEI, Linear, MW 25,000; Polysciences, Hirschberg, Germany), 100 mg/l in 0.1 mmol/l NaCl, pH 7.8. 412.5 µl of PEI was mixed with different concentrations of the AONs. Polyplexes formed during 10 minutes at room temperature and were later dispersed into the cell culture flasks to a final volume of 7.5 ml per T25 flask. For the PEI-based transfections, the cells were incubated with the oligonucleotide/polyplexes for 6 hours in DMEM supplemented with 10% FCS (DMEM/FCS). After 6 hours the transfection medium was replaced by fresh DMEM/FCS/Pen-Strep medium. Cells were harvested at different time points, using the Peq Gold total RNA kit (Peqlab, Erlangen, Germany), followed by complementary DNA (cDNA) synthesis with the Transcriptor High Fidelity cDNA Synthesis Kit (Roche, Mannheim, Germany).

RT-PCR and pyrosequencing. cDNA from AON-treated biological triplicates was PCR-amplified using a set of primers that specifically amplifies correctly spliced exon 4b– exon 5 junctions. For relative quantification of paternal and maternal (mutant) allele-derived transcripts we performed pyrosequencing of a common heterozygous SNP in exon 4 (rs7624750) on RT-PCR products (**Figure 3** and **Supplementary Figure S2**). Pyrosequencing assay primers were created using the PyroMark Assay Design 2.0 software (Qiagen, Hilden, Germany): N158S-forward (5′-TGGATTGTGCCTGACATTGT-3′), N158S-biot-reverse (5′-(BTN) CCGTTTCTTCCGGAGAACCTAA-3′), and N158S-seq (5′-TTAGAAAAGCCCTTCCT-3′). Pyrosequencing was carried out using the PyroMark Q96 ID instrument (Qiagen), while the sample preparation and the data analysis were performed according to the manufacturer's instruction.

Western blot. For semiquantitative determination of the amount of OPA1 protein, we performed Western blotting experiments with whole cell lysates using antibodies against OPA1 (BD Biosciences, Heidelberg, Germany, Cat.: 612607), HSP60 (Enzo Life Sciences, Lörrach, Germany, Cat.: ADI-SPA-806-D), and BETA-ACTIN (Merck-Millipore, Darmstadt, Germany, Cat.: MAB1501). A fluorescent-labeled antimouse antibody (LI-COR Biosciences, Bad Homburg, Germany, Cat. 926–32210) was used for signal detection and quantification on an Odyssey Sa instrument (LI-COR Biosciences).

Statistical analysis. Statistical software (SPSS 15; SPSS, Chicago, IL) was used for all the statistical analyses. The Kolmogorov–Smirnov test was used to confirm the normality of the data. The homogeneity of the variances was assessed with Levene's test. To determine concentration dependent AON-effects, factorial analysis of variance tests were performed. One-way analysis of variance tests were used to analyze the AON effect through time. To detect differences between specific time points, post hoc tests were performed. Student's *t*-tests (normal distribution and homoscedasticity of the data) or *U*-Mann–Whitney test (normal distribution and no homoscedasticity of the data) were used when comparing two groups. All data are presented as mean ± SD. $P < 0.05$ was considered statistically significant ($P < 0.05$ (*), $P < 0.01$ (**), $P < 0.001$ (***), $P < 0.0001$ (****). Graphs were calculated using Sigma-Plot 13 (Systat Software GmbH, Erkrath, Germany).

Supplementary material

Figure S1. Frameshifting by inclusion of cryptic exon c and c+.
Figure S2. Pyrosequencing assay for rs7624750.
Table S1. Off-targets for AC AON and BP AON.

Acknowledgments We thank the patients and their family members for donating fibroblasts for our study, the Tübingen Dermatology department for technological support, especially Christina Braunsdorf for introduction and advice to the Li-Cor Odyssey instrument. We are grateful to Caroline Schönfeld for skillful technical support in cell culture experiments. Special thanks to Juan Luis Mateo Cerdan, Center for Organismal Studies, Heidelberg, for customizing the off-target search using CCtop. This work was funded, in part, by the BMBF (ERARE JTC "PREPARE", Kz. 01GM1607, to M.S.) and the mitoNET grant (01GM1113E to L.S.). The authors report that there are no conflicts of interest.

1. Alexander, C, Votruba, M, Pesch, UE, Thiselton, DL, Mayer, S, Moore, A *et al.* (2000). OPA1, encoding a dynamin-related GTPase, is mutated in autosomal dominant optic atrophy linked to chromosome 3q28. *Nat Genet* **26**: 211–215.
2. Delettre, C, Lenaers, G, Griffoin, JM, Gigarel, N, Lorenzo, C, Belenguer, P *et al.* (2000). Nuclear gene OPA1, encoding a mitochondrial dynamin-related protein, is mutated in dominant optic atrophy. *Nat Genet* **26**: 207–210.
3. Anikster, Y, Kleta, R, Shaag, A, Gahl, WA and Elpeleg, O (2001). Type III 3-methylglutaconic aciduria (optic atrophy plus syndrome, or Costeff optic atrophy syndrome): identification of the OPA3 gene and its founder mutation in Iraqi Jews. *Am J Hum Genet* **69**: 1218–1224.
4. Hanein, S, Perrault, I, Roche, O, Gerber, S, Khadom, N, Rio, M *et al.* (2009). TMEM126A, encoding a mitochondrial protein, is mutated in autosomal-recessive nonsyndromic optic atrophy. *Am J Hum Genet* **84**: 493–498.
5. Metodiev, MD, Gerber, S, Hubert, L, Delahodde, A, Chretien, D, Gérard, X *et al.* (2014). Mutations in the tricarboxylic acid cycle enzyme, aconitase 2, cause either isolated or syndromic optic neuropathy with encephalopathy and cerebellar atrophy. *J Med Genet* **51**: 834–838.
6. Inoue, H, Tanizawa, Y, Wasson, J, Behn, P, Kalidas, K, Bernal-Mizrachi, E *et al.* (1998). A gene encoding a transmembrane protein is mutated in patients with diabetes mellitus and optic atrophy (Wolfram syndrome). *Nat Genet* **20**: 143–148.
7. Chaussenot, A, Rouzier, C, Quere, M, Plutino, M, Ait-El-Mkadem, S, Bannwarth, S *et al.* (2015). Mutation update and uncommon phenotypes in a French cohort of 96 patients with WFS1-related disorders. *Clin Genet* **87**: 430–439.
8. Angebault, C, Guichet, PO, Talmat-Amar, Y, Charif, M, Gerber, S, Fares-Taie, L *et al.* (2015). Recessive mutations in RTN4IP1 cause isolated and syndromic optic neuropathies. *Am J Hum Genet* **97**: 754–760.
9. Elachouri, G, Vidoni, S, Zanna, C, Pattyn, A, Boukhaddaoui, H, Gaget, K *et al.* (2011). OPA1 links human mitochondrial genome maintenance to mtDNA replication and distribution. *Genome Res* **21**: 12–20.
10. Frezza, C, Cipolat, S, Martins de Brito, O, Micaroni, M, Beznoussenko, GV, Rudka, T *et al.* (2006). OPA1 controls apoptotic cristae remodeling independently from mitochondrial fusion. *Cell* **126**: 177–189.
11. Cipolat, S, Martins de Brito, O, Dal Zilio, B and Scorrano, L (2004). OPA1 requires mitofusin 1 to promote mitochondrial fusion. *Proc Natl Acad Sci USA* **101**: 15927–15932.
12. Marchbank, NJ, Craig, JE, Leek, JP, Toohey, M, Churchill, AJ, Markham, AF *et al.* (2002). Deletion of the OPA1 gene in a dominant optic atrophy family: evidence that haploinsufficiency is the cause of disease. *J Med Genet* **39**: e47.
13. Yu-Wai-Man, P, Griffiths, PG, Burke, A, Sellar, PW, Clarke, MP, Gnanaraj, L *et al.* (2010). The prevalence and natural history of dominant optic atrophy due to OPA1 mutations. *Ophthalmology* **117**: 1538–46, 1546.e1.
14. Bonifert, T, Karle, KN, Tonagel, F, Batra, M, Wilhelm, C, Theurer, Y *et al.* (2014). Pure and syndromic optic atrophy explained by deep intronic OPA1 mutations and an intralocus modifier. *Brain* **137**(Pt 8): 2164–2177.
15. Sharma, VK and Watts, JK (2015). Oligonucleotide therapeutics: chemistry, delivery and clinical progress. *Future Med Chem* **7**: 2221–2242.
16. Anderson, KP, Fox, MC, Brown-Driver, V, Martin, MJ and Azad, RF (1996). Inhibition of human cytomegalovirus immediate-early gene expression by an antisense oligonucleotide complementary to immediate-early RNA. *Antimicrob Agents Chemother* **40**: 2004–2011.
17. Crooke, RM, Graham, MJ, Lemonidis, KM, Whipple, CP, Koo, S and Perera, RJ (2005). An apolipoprotein B antisense oligonucleotide lowers LDL cholesterol in hyperlipidemic mice without causing hepatic steatosis. *J Lipid Res* **46**: 872–884.
18. Voit, T, Topaloglu, H, Straub, V, Muntoni, F, Deconinck, N, Campion, G *et al.* (2014). Safety and efficacy of drisapersen for the treatment of Duchenne muscular dystrophy (DEMAND II): an exploratory, randomised, placebo-controlled phase 2 study. *Lancet Neurol* **13**: 987–996.
19. Mendell, JR, Goemans, N, Lowes, LP, Alfano, LN, Berry, K, Shao, J *et al.*; Eteplirsen Study Group and Telethon Foundation DMD Italian Network. (2016). Longitudinal effect of eteplirsen versus historical control on ambulation in Duchenne muscular dystrophy. *Ann Neurol* **79**: 257–271.
20. Collin, RW, den Hollander, AI, van der Velde-Visser, SD, Bennicelli, J, Bennett, J and Cremers, FP (2012). Antisense oligonucleotide (AON)-based therapy for Leber congenital amaurosis caused by a frequent mutation in CEP290. *Mol Ther Nucleic Acids* **1**: e14.
21. Gerard, X, Perrault, I, Hanein, S, Silva, E, Bigot, K, Defoort-Delhemmes, S *et al.* (2012). AON-mediated exon skipping restores ciliation in fibroblasts harboring the common Leber congenital amaurosis CEP290 mutation. *Mol Ther Nucleic Acids* **1**: e29.
22. Piotrovskii, VK (1987). Pharmacokinetic stochastic model with Weibull-distributed residence times of drug molecules in the body. *Eur J Clin Pharmacol* **32**: 515–523.
23. Carrasco, RA, Stamm, NB, Marcusson, E, Sandusky, G, Iversen, P and Patel, BK (2011). Antisense inhibition of survivin expression as a cancer therapeutic. *Mol Cancer Ther* **10**: 221–232.
24. Aartsma-Rus, A, De Winter, CL, Janson, AA, Kaman, WE, Van Ommen, GJ, Den Dunnen, JT *et al.* (2005). Functional analysis of 114 exon-internal AONs for targeted DMD exon skipping: indication for steric hindrance of SR protein binding sites. *Oligonucleotides* **15**: 284–297.
25. Singh, NK, Singh, NN, Androphy, EJ and Singh, RN (2006). Splicing of a critical exon of human survival motor neuron is regulated by a unique silencer element located in the last intron. *Mol Cell Biol* **26**: 1333–1346.
26. Bassi, E, Falzarano, S, Fabris, M, Gualandi, F, Merlini, L, Vattemi, G *et al.* (2012). Persistent dystrophin protein restoration 90 days after a course of intraperitoneally administered naked 2'OMePS AON and ZM2 NP-AON complexes in mdx mice. *J Biomed Biotechnol* **2012**: 897076.
27. Gérard, X, Perrault, I, Munnich, A, Kaplan, J and Rozet, JM (2015). Intravitreal injection of splice-switching oligonucleotides to manipulate splicing in retinal cells. *Mol Ther Nucleic Acids* **4**: e250.
28. Garanto, A, Chung, DC, Duijkers, L, Corral-Serrano, JC, Messchaert, M, Xiao, R *et al.* (2016). *In vitro* and *in vivo* rescue of aberrant splicing in CEP290-associated LCA by antisense oligonucleotide delivery. *Hum Mol Genet* (epub ahead of print).
29. Singh, NN, Lee, BM and Singh, RN (2015). Splicing regulation in spinal muscular atrophy by an RNA structure formed by long-distance interactions. *Ann NY Acad Sci* **1341**: 176–187.
30. Zalachoras, I, Evers, MM, van Roon-Mom, WM, Aartsma-Rus, AM and Meijer, OC (2011). Antisense-mediated RNA targeting: versatile and expedient genetic manipulation in the brain. *Front Mol Neurosci* **4**: 10.
31. Garanto, A, van Beersum, SE, Peters, TA, Roepman, R, Cremers, FP and Collin, RW (2013). Unexpected CEP290 mRNA splicing in a humanized knock-in mouse model for Leber congenital amaurosis. *PLoS One* **8**: e79369.
32. Aartsma-Rus, A, van Vliet, L, Hirschi, M, Janson, AA, Heemskerk, H, de Winter, CL *et al.* (2009). Guidelines for antisense oligonucleotide design and insight into splice-modulating mechanisms. *Mol Ther* **17**: 548–553.
33. Zuker, M (2003). Mfold web server for nucleic acid folding and hybridization prediction. *Nucleic Acids Res* **31**: 3406–3415.
34. Hofacker, IL (2003). Vienna RNA secondary structure server. *Nucleic Acids Res* **31**: 3429–3431.

35. Desmet, FO, Hamroun, D, Lalande, M, Collod-Béroud, G, Claustres, M and Béroud, C (2009). Human splicing finder: an online bioinformatics tool to predict splicing signals. *Nucleic Acids Res* **37**: e67.
36. Langmead, B, Trapnell, C, Pop, M and Salzberg, SL (2009). Ultrafast and memory-efficient alignment of short DNA sequences to the human genome. *Genome Biol* **10**: R25.
37. Stemmer, M, Thumberger, T, Del Sol Keyer, M, Wittbrodt, J and Mateo, JL (2015). CCTop: an intuitive, flexible and reliable CRISPR/Cas9 target prediction tool. *PLoS One* **10**: e0124633.
38. Aartsma-Rus, A, Kaman, WE, Bremmer-Bout, M, Janson, AA, den Dunnen, JT, van Ommen, GJ *et al.* (2004). Comparative analysis of antisense oligonucleotide analogs for targeted DMD exon 46 skipping in muscle cells. *Gene Ther* **11**: 1391–1398.

Supplementary Information accompanies this paper on the Molecular Therapy–Nucleic Acids website (http://www.nature.com/mtna)